Bull. Mater. Sci., Vol. 37, No. 7, December 2014, pp. 1583–1588. © Indian Academy of Sciences.

Optimization of nanocrystalline γ-alumina coating for direct spray water-cooling of optical devices

S N ALAM[1,2,*], M ANARAKY[3], Z SHAFEIZADEH[3] and P J PARBROOK[1]

[1]Tyndall National Institute, University College Cork, Lee Maltings, Dyke Parade, Cork, Ireland
[2]Physics Department, Iran University of Science and Technology, P.O. Box 16765-163, Tehran, Iran
[3]Iranian Laser Science and Technology Center, P.O. Box 14655-576, Tehran, Iran

MS received 8 May 2013; revised 7 February 2014

Abstract. **In this study, aluminium oxide films were deposited on BK7 glass substrates using radio frequency magnetron sputtering. The purposes of this study are to clarify the influence of O_2 flow as reactive partial gas, which is necessary to form Al_2O_3 films, and then the influence of substrate temperature on structure and rigidity of coatings towards water injection. The fabricated metal oxide films were characterized using techniques such as atomic force microscopy (AFM), X-ray diffraction (XRD), spectrophotometry, ellipsometry and Rutherford backscattering (RBS) analysis. Modifications of the partial gas percentage influences the optical properties and composition of the deposited aluminium oxide, the best samples being those deposited with 5% and 8% oxygen. The substrate temperature affects the structure and crystallization of the films. Nanocrystalline γ-Al_2O_3 has been observed at temperatures above 300 °C with the grain size of 25 nm. After water injection, there was a large diversity in the surface roughness of samples with different substrate temperature. Experiments have shown that the best resistance against water injection occurs for the sample deposited at 350 °C with 5% partial gas. We conclude that the rigidity of nanocrystalline γ-Al_2O_3 coatings can be explained by both Hall–Petch and Coble creep mechanism. In this case, there is an optimum grain size of around 42 nm against water spray.**

Keywords. **Aluminium oxide; magnetron sputtering; nanocrystalline; water cooling; Hall–Petch model; Coble creep mechanism.**

1. Introduction

Aluminum oxide (alumina, Al_2O_3) is currently one of the most useful oxide ceramics, as it has been used in many fields of engineering such as optical coatings, heat-resistant materials, abrasive grains and cutting materials. Al_2O_3 films have been deposited using sol gel (Bahlawane and Watanabe 2000), CVD (Ritala *et al* 1999; Groner *et al* 2004), evaporation (Hoffman and Leibowitz 1971) and sputtering (Jin *et al* 2003). On the other hand, aluminum oxide layer could be useful for coating the spray water-cooled optical and electrical devices, due to its interesting properties such as optical transparency, high rigidity, high thermal conductivity (58 W/m-K at 250 K) and low thermal expansion ($\sim 7 \times 10^{-6}$ K) (Weber 2003). Spray water cooling is an important technique used for cooling in modern industrial and technological applications, such as cooling of electronic components and the use of high power lasers (Jia and Qiu 2003; Hidrovo and Goodson 2008; Weiwei and Gomez 2011), to remove the heat introduced by the laser (Treusch *et al* 2005; Bar-Cohen *et al* 2006). However, the formation of high quality Al_2O_3 films usually requires a high substrate temperature, well around 400 °C for physical vapour deposition (Groner *et al* 2002).

These high-temperature requirements limit the number of usable substrate materials and, therefore, the application range for Al_2O_3 thin films. High quality Al_2O_3 layers were reported at a low substrate temperature, as low as 400 °C using Cr_2O_3 template (Jin *et al* 2003) and combination of ionised and pulsed DC sputtering (Zywistzki and Hoetzsch 1996) at ~350 °C.

In this study, aluminum oxide films were deposited using conventional RF magnetron sputtering and the influence of O_2 flow in the Ar ambient and substrate temperature on structure and properties of coatings have been investigated to clarify the influence of reactive gas and temperature. In this experiment, a spray-water system was used to simulate the water cooling condition and to understand the effect of water jet droplets on alumina films, as a rigid and heat exchanging layer.

2. Materials and methods

Aluminium Oxide films were deposited by RF reactive magnetron sputtering technique. BK7 circular glass plates of 2 mm thickness and 30 mm diameter with surface flatness of $\lambda/10@633$ nm were used as substrates. The target was an Al_2O_3 plate with 99·999% purity, which deposited on substrates under conditions that will be explained subsequently.

*Author for correspondence (shahab.norouzian@tyndall.ie)

Initially, the substrates were ultrasonically cleaned in 0·02 M HCl acetone and immersed in deionised water, then dried by N_2 and transferred immediately to the coating chamber. Pre-ion cleaning was performed to improve the adhesion between layer and substrate. Next, the sputter chamber was evacuated to $1{\cdot}5 \times 10^{-7}$ Torr and deposition was started by injecting an oxygen and argon gas mixture of composition given by $(O_2/(O_2+Ar)\%)$. Various O_2 percentages and then different substrate temperatures of 200, 300, 350 and 400 °C were investigated. The sputtering conditions of Al_2O_3 films are given in table 1.

For simplicity, the samples were coded as shown in table 2.

The prepared coatings were characterized using atomic force microscopy (AFM) non-contact mode (Dual Scope DME SPM), X-ray diffraction, spectrophotometry (Varian Cary 6000i UV-visible-NIR) and ellipsometry. The elemental composition (at.%) of the films were determined using Rutherford backscattering spectroscopy (RBS). The computer program SIMNRA was used to interpret the results. The films were analyzed using 2·0 MeV He^+ ions at normal incidence at a 165° detection angle. The spray water system used for this experiment was based on a water pump, a filter and a spray head with one nozzle. The high pressure (50 bar) water was filtered and then sprayed by a head mounting nozzle for 48 h. An electronic analytical balance, having the accuracy of ±0·01 mg, was used to weigh the samples.

3. Results and discussion

Measurements of thickness modifications according to changes of the percentage of oxygen reactive gas are shown in figure 1. It was observed that by increasing $(O_2/(O_2+Ar)\%)$, the thickness of the layer was reduced. It is believed that the lower sputtering yield of oxygen upon replacing argon can lead partly to a decrease of aluminum sputtered atoms which causes a decrease in thickness of the as deposited films.

A typical RBS spectrum of the A2 sample is shown in figure 2.

The stoichiometry of the sputtered AlO_x (where x is the O/Al atomic ratio) films was determined by RBS measurements. The RBS results show that the oxygen and aluminum content in the layers is influenced by proportion of O_2 in the sputtering gases during deposition. Stoichiometry of films, which were synthesized with various oxygen concentrations, changed from under-stoichiometry ($x < 3/2$) to

Table 1. Deposition conditions of alumina films.

Sputtering target	Al_2O_3
Target purity	99·999 %
Substrate	BK7
Target to substrate distance (cm)	10
Working pressure (Torr)	$4{\cdot}8 \times 10^{-3} - 4{\cdot}9 \times 10^{-3}$
$O_2/(O_2+Ar)\%$	3, 5, 8, 12
Sputtering power (W)	500 (RF)
Substrate temperature (°C)	200, 300, 350, 400

Table 2. Coded samples deposited in different conditions.

Sample code	Sub. temp. (°C)	$O_2/(O_2+Ar)\%$	Sp. time (min)
A1	200	3	60
A2	200	5	60
A3	200	8	60
A4	200	12	60
B1	200	5	150
B2	300	5	150
B3	350	5	150
B4	400	5	150

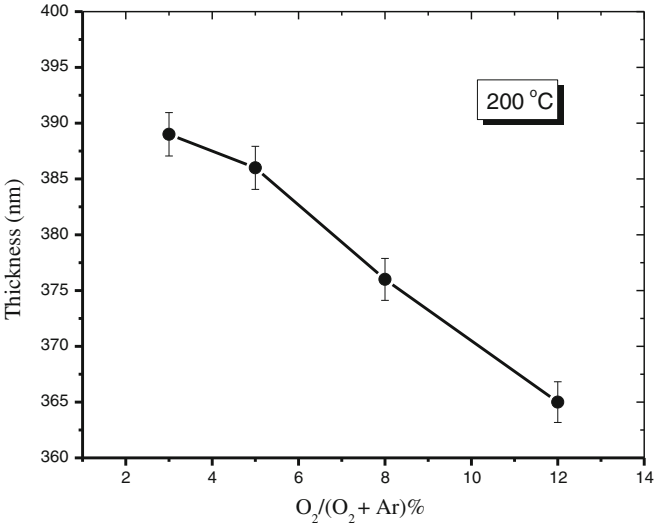

Figure 1. Variation of films thickness as a function of oxygen volume percentage at 200 °C.

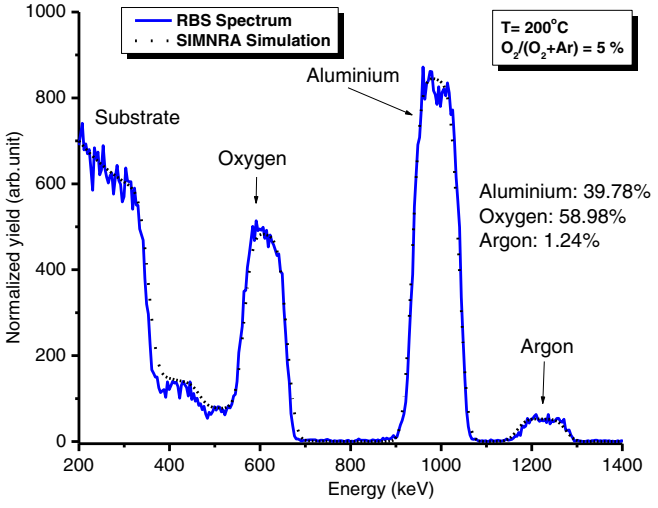

Figure 2. Typical RBS spectrum with corresponding SIMNRA simulated curve.

over-stoichiometry ($x > 3/2$) (figure 3). Variation of oxygen concentration in aluminum oxide was also reported by some other researchers (Ortiz *et al* 2000; Klie *et al* 2003).

As observed from the compositional studies, the O/Al ratio is nearly approaching stoichiometry of 3/2 for sample A2. So, it is possible to prepare reproducible high quality Al_2O_3. Additionally, all the films contained ~1% Ar as determined by the RBS measurement. Furthermore, the ellipsometry analysis reveals that the refractive indexes of those samples deposited under 5% and 8% $O_2/(O_2+Ar)$% are around 1·55, which well agreed with high quality Al_2O_3 (Hoffman and Leibowitz 1971; Groner *et al* 2004).

After optimization of oxygen proportion in sputtering gas for deposition Al_2O_3 films, the effect of substrate temperature on the crystal properties of aluminum oxide were investigated by fixing the $O_2/(O_2+Ar)$% at 5%. The X-ray diffraction patterns of the films deposited on the substrate held at 200, 300, 350 and 400 °C and fixed reactive gas flow ratio are shown in figure 4.

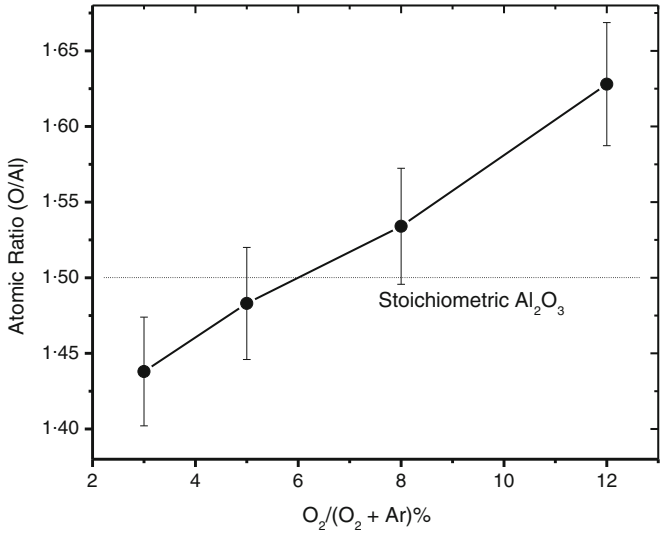

Figure 3. Compositional change of alumina thin films as a function of oxygen flow ratio.

It is seen in the XRD pattern of sample B1 that there is no peak indicative of crystallinity or, at least, it is not identifiable with our XRD system. Hence, the deposited film at 200 °C is assumed to be in an amorphous state. The amorphous background can be attributed to two sources: (1) the contribution from the BK7 substrate; and (2) the fact that the films may be partly amorphous due to the low substrate temperature during deposition. The emergence of an amorphous-crystalline phase transformation is observed at 300 °C. The films deposited at 300 °C showed the presence of a weak peak of the γ-Al_2O_3 phase (Chupas *et al* 2001; Rozita *et al* 2010). This crystalline phase becomes more pronounced at a temperature of 350 °C. As the substrate temperature is increased from 350 to 400 °C, the (2 2 0) peak intensity rapidly rises with a corresponding to decreases in the full-width at half-maximum (FWHM), indicating a strong increase in crystallinity.

Crystallite size is actually determined by measuring the broadening of a particular X-ray diffraction (XRD) peak in a diffraction pattern and the grain size calculation by XRD has been confirmed by a number of groups using TEM images (Guerrero-Paz and Jaramillo 1999; Borchert *et al* 2005; Blennow *et al* 2008). Therefore, in this work, the grain sizes of the deposited samples calculated from the XRD data using Scherrer formulae (Patterson 1939):

$$D = \frac{K\lambda}{\beta \cos\theta_0} \tag{1}$$

where λ is the wavelength of the X-ray radiation (λ = 1·541 Å), K the Scherrer constant ($K \approx 0{\cdot}89$), θ_0 the Bragg diffraction angle and β the FWHM of the (2 2 0) plane (in radians).

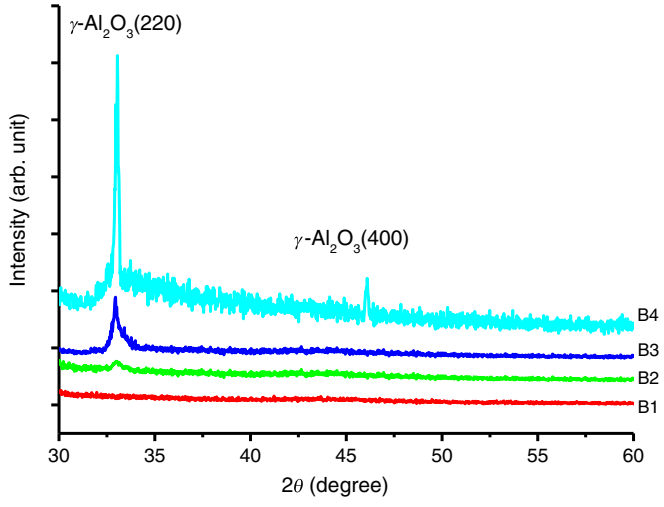

Figure 4. X-ray diffraction patterns of alumina films deposited at different substrate temperatures.

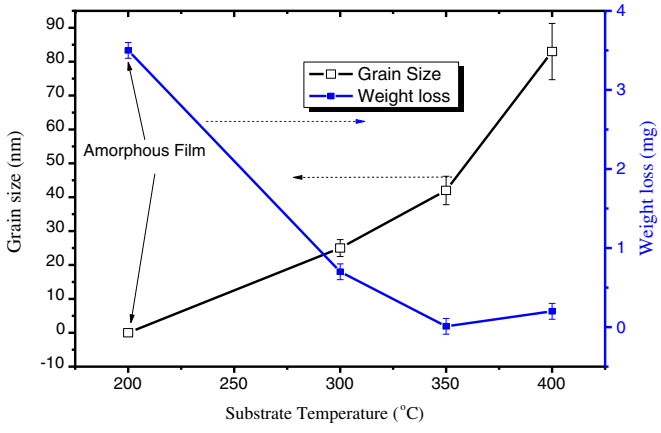

Figure 5. Grain size and weight loss of the films as a function of substrate temperature.

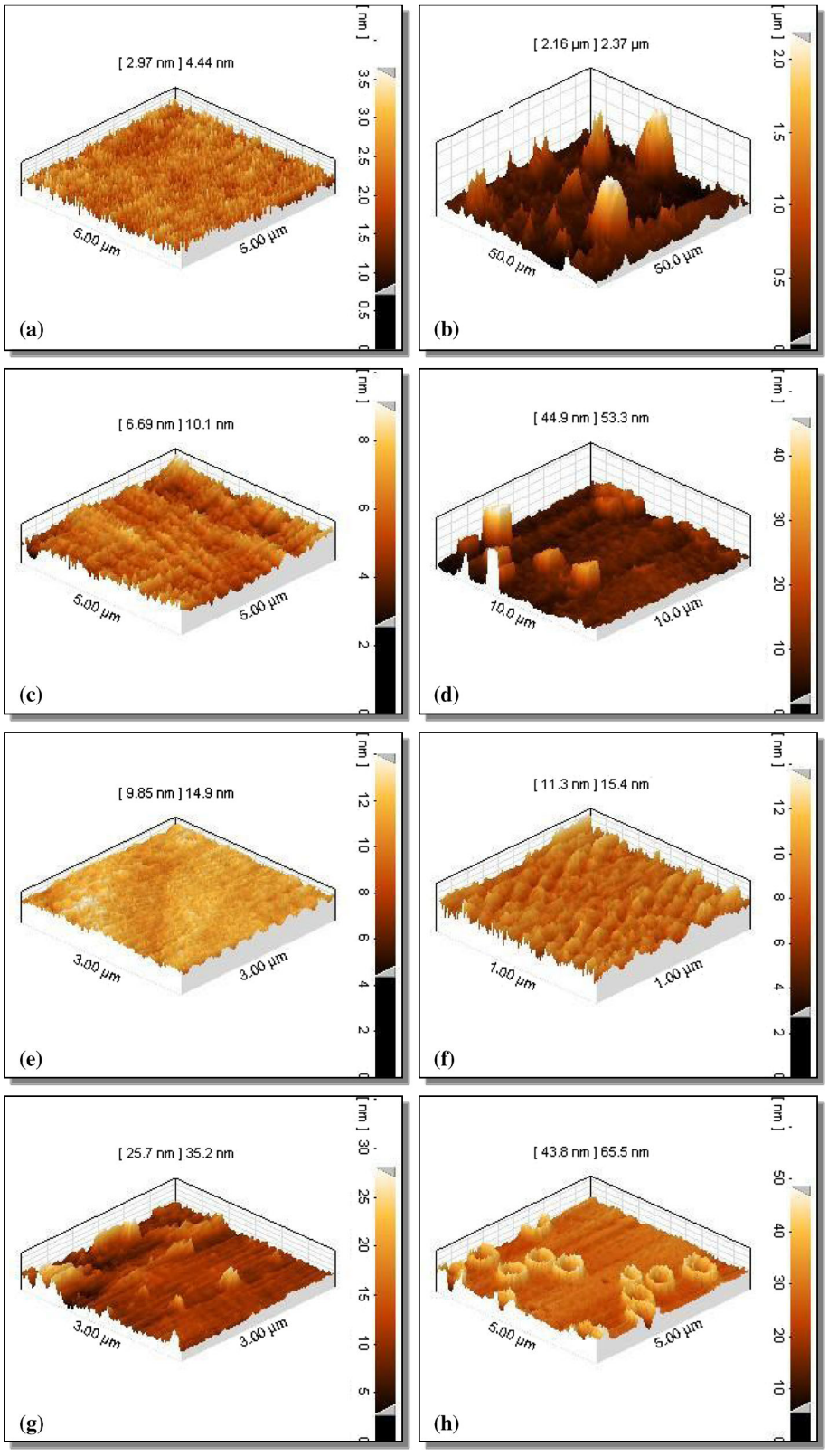

Figure 6. AFM images of B1 (200 °C), B2 (300 °C), B3 (350 °C) and B4 (400 °C) samples before and after spray-water test: (**a**) B1 before test, (**b**) B1 after test (**c**) B2 before test, (**d**) B2 after test, (**e**) B3 before test, (**f**) B3 after test, (**g**) B4 before test and (**h**) B4 after test.

Table 3. RMS roughness of samples before and after water test.

Sample		B1	B2	B3	B4
Roughness (nm)	Before test	2·97	6·69	9·85	25·7
	After test	~2160	44·9	11·3	43·8

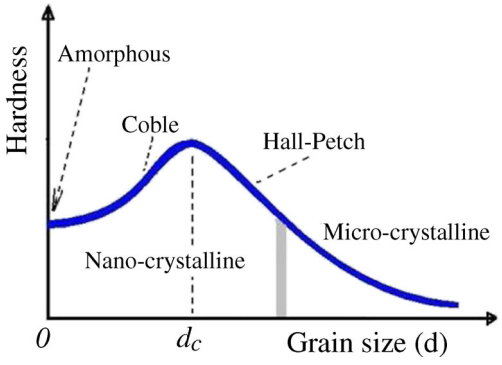

Figure 7. Schematic illustration of hardness vs average grain size.

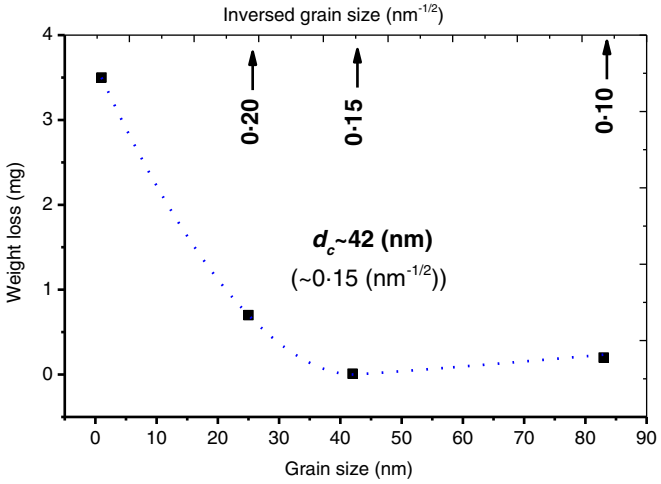

Figure 8. Weight loss of Al_2O_3 coatings as a function of average grain size.

The grains appear to grow with increment of substrate temperature, from 25 to 42 and 83 nm for B2, B3 and B4 samples, respectively.

The spray water system was used to evaluate the influence of substrate temperature on the rigidity of coatings towards water injection.

Figure 5 illustrates the weight loss and grain size of layers as a function of substrate temperature. It can be observed that amorphous sample had highest weight loss, which could be due to the removal of all top layers after the water test. The loss decreased with increase in grain size up to 42 nm. Then, on increasing the grain size up to 83 nm for the sample deposited at a temperature of 400 °C, there was a slightly higher weight loss.

In order to assess the surface roughness and gain more understanding about what was happening on alumina films during droplet impingements, AFM non-contact mode was utilized before and after the spray-water test. Figure 6 depicts the 3D AFM image of the B1, B2, B3 and B4 films before and after test. The topography investigations of the as-deposited samples with different substrate temperature show quite different characteristics. The roughnesses (root mean square (RMS) deviation) of samples are presented in table 3.

The surface roughness shows an increase with respect to the substrate temperature. It also shows that the films are uniform with nano-sized grains. Figure 6(b, d, f and h) illustrate the AFM image of samples after water-spray test. These micrographs show erosion after the test cycle on account of the impingement of droplets. The high velocity, high pressure water spray not only cools the surface of material, but also attacks the microstructure of the coating. Noticeably, there are several pits on the surface of sample B4 (figure 6h), and the least changes are observed on the surface of B3 (figure 6f), deposited at 350 °C.

The mechanical properties of polycrystalline metals and alloys are very sensitive to their grain size. It has been recognized that the strength of a polycrystalline material can be effectively increased by modifiying its grain size (Wang *et al* 1995).

Conventionally mechanical behaviour of multicrystalline materials based upon dislocations can be explained by the Hall–Petch equation:

$$H = H_0 + kd^{-1/2}, \tag{2}$$

where H is the hardness of layer, H_0 and k are constants and d the average grain size. But, at very small grain sizes, the Hall–Petch model may not be operative. In this region, Chokshi *et al* (1989) have proposed the Coble creep mechanism to explain mechanical behaviour of nanocrystalline material below a critical grain size, d_c:

$$H = A + Bd^3, \tag{3}$$

where A and B are constants depending on material properties.

Material hardness as a function of average grain size is schematically illustrated in figure 7.

If it is assumed that weight loss has inverted relation to film hardness, summarizing the topographic and weight-loss experiments leads us to conclude that stiffness of our nanocrystalline γ-Al_2O_3 coatings followed the Coble creep mechanism of hardness vs the average grain size until the grain size increased to about 42 nm ($d^{-1/2} \approx 0{\cdot}15\,\text{nm}^{-1/2}$). At higher grain size (83 nm), Coble creep compromised and even exhibited higher hardness, following the conventional Hall–Petch relation (figure 8). In this case, the critical size

($d_c^{-1/2}$) for nanocrystalline alumina films, to converting the Hall–Petch into Coble creep mechanism would be around $0{\cdot}15\,\mathrm{nm}^{-1/2}$.

This behaviour of nanocrystalline materials was explained by a number of researchers (Takeuchi 2001; Meyers *et al* 2006; Carlton and Ferreira 2007).

Additionally, thermodynamically stable films determine the relative stability of the overall system. Thus, another reason for softening the coatings deposited at 350 °C and less can be due to lower γ-Al_2O_3 (220) intensity and then lower chemical stability, leading to degradation of the phase stability (Larijani *et al* 2009).

4. Conclusions

Effects of oxygen flow ratio and substrate temperature have been investigated on the structure and properties of aluminum oxide films deposited using RF magnetron sputtering. Experiments show that, in the structural point of view, the best samples are those deposited with 5 and 8 oxygen percentages. It is revealed that nanocrystalline γ-Al_2O_3 can be grown at a temperature as low as 300 °C. After water injection, the surface roughness of samples were varied with regard to different substrate temperature. Moreover, experiments have shown that the layer which deposited in condition of 5% oxygen flow ratio and substrate temperature of 350 °C has the best resistance against spray water injection.

Finally, we conclude that the stiffness of the nanocrystalline γ-Al_2O_3 coatings against water spray can be explained by both Hall–Petch and Coble creep mechanisms. In this case, there is an optimum grain size of around 42 nm.

References

Bahlawane N and Watanabe T 2000 *J. Am. Ceram. Soc.* **83** 2324

Bar-Cohen A, Arik M and Ohadi M 2006 *Proc. IEEE* **94** 1549

Blennow P, Hansen K K, Wallenberg L R and Mogensen M 2008 *ECS Transactions* **13** 181

Borchert H, Shevchenko E V and Robert A 2005 *Langmuir* **21** 1931

Carlton C E and Ferreira P J 2007 *Acta Mater.* **55** 3749

Chokshi A H, Rosen A, Karch J and Gleiter H 1989 *Scripta Metall. Mater.* **23** 1679

Chupas P J, Ciraolo M F, Hanson J C and Grey C P 2001 *J. Am. Chem. Soc.* **123** 1694

Groner M D, Elam J W, Fabreguette F H and George S M 2002 *Thin Solid Films* **413** 186

Groner M D, Fabreguette F H, Elam J W and George S M 2004 *Chem. Mater.* **16** 639

Guerrero P J and Jaramillo V D 1999 *Nanostruct. Mater.* **11** 1195

Hidrovo C and Goodson K E 2008 *Electrical, optical and thermal interconnections for 3D integrated systems* (eds) J Meindl and M Bakir (Boston: Artech) p 293

Hoffman D and Leibowitz D 1971 *J. Vac. Sci. Technol.* **8** 107

Jia W and Qiu H-H 2003 *Exp. Therm. Fluid Sci.* **27** 829

Jin P, Nakao S, Wang S X and Wang L M 2003 *Appl. Phys. Lett.* **82** 1024

Klie R F, Browning N D, Chowdhuri A R and Takoudis C G 2003 *Appl. Phys. Lett.* **83** 1187

Larijani M M, Norouzian Sh, Afzalzadeh R, Balashabadi P and Dibaji H 2009 *Surf. Coat. Tech.* **203** 2486

Meyers M A, Mishra A and Benson D J 2006 *Prog. Mater. Sci.* **51** 427

Ortiz A, Alonso J C, Pankov V, Huanosta A and Andrade E 2000 *Thin Solid Films* **368** 74

Patterson A L 1939 *Phys. Rev.* **56** 978

Ritala M, Leskelä M, Dekker J P, Mutsaers C, Soininen P J and Skarp J 1999 *Chem. Vap. Depos.* **5** 7

Rozita R, Brydson R and Scott A J 2010 *J. Phys.: Conference Series* **241** 012096

Takeuchi S 2001 *Scripta Mater.* **44** 1483

Treusch G, Srinivasan R, Brown D, Miller R and Harrison J 2005 *Proc. SPIE* (Bellingham, WA: SPIE) 5711

Wang N, Wang Z, Aust K T and Erb U 1995 *Acta Metall. Mater.* **43** 519

Weber M J 2003 *Handbook of optical materials* (Berkeley, California: CRC Press)

Weiwei D and Gomez A 2011 *Int. J. Heat Mass Tran.* **54** 2270

Zywistzki O and Hoetzsch G 1996 *Surf. Coat. Tech.* **86** 640